Sub-μm air-gap resonant MEMS mass sensors fabrication and electrical characterization for the detection of airborne particles

Ugur Soysal, Frédéric Marty, Emmanuelle Algre, Evelyne Gehin, Charles Motzkus

Sub-µm air-gap resonant MEMS mass sensors fabrication and electrical characterization for the detection of airborne particles

Ugur Soysal
CERTES (EA3481)
Université Paris-Est
94010 Creteil Cedex, France
ugur.soysal@u-pec.fr

Frédéric Marty
ESYCOM (EA 2552)
ESIEE Paris, Université Paris-Est
93162 Noisy Ie Grand Cedex, France
frederic.marty@esiee.fr

Emmanuelle Algré
ESYCOM (EA 2552)
ESIEE Paris, Université Paris-Est
93162 Noisy Ie Grand Cedex, France
emmanuelle.algre@esiee.fr

Evelyne Géhin
CERTES (EA3481)
Université Paris-Est
94010 Creteil Cedex, France
gehin@u-pec.fr

Charles Motzkus
CSTB
77447 Marne-la-Vallee Cedex 2, France
charles.motzkus@cstb.fr

***Abstract*— As excessive exposure to airborne particles results in adverse health effects, the development of a real-time aerosol monitoring system is highly relevant. Widely used systems are bulky, time consuming, labor intensive or expensive to maintain. Based on the airborne particle detection capacities of micro sensors, typical acoustic wave mass sensors such as the Surface Acoustic Wave (SAW), the Film Bulk Acoustic Resonator (FBAR), and the Quartz Crystal Microbalance (QCM) sensors show lack of mass sensitivity and uniformity. However, resonant MEMS sensors show good sensitivity and could be relevant alternatives to typical acoustic wave mass sensors for low mass measurements [1]. Among the various types of bulk mode MEMS resonant transduction methods, capacitively transduced MEMS resonators show sensitive and relatively uniform mass measurements [2]. Herein, we propose the thick oxide mask layer fabrication technique to realize high performance mass sensors. This fabrication technique was previously proposed for reducing resonator-to-electrode gaps to sub-µm [3]. In this study, we used the thick oxide mask layer technique to fabricate high aspect ratio sub-µm air-gap MEMS mass sensors. We obtained the mean gap size as ~ 868 nm for 40 µm thick resonators. Preliminary electrical characterization results showed that the resonance frequency of the resonators is 4.409 MHz, and the quality factor is estimated as 15303.**

Keywords—MEMS, real-time detection, microbalance, sub-µm air gap, airborne particles

I. INTRODUCTION

Sophisticatedly designed MEMS mass sensors can be integrated to an inexpensive, portable, and low power consumption real-time aerosol monitoring system. Among MEMS devices, bulk mode single-crystal silicon (SCS) MEMS resonant devices come to the forefront due to their superior Q-factor, resonance frequency, and tunable surface area [4][5][6]. Unlike typical acoustic wave resonators, when MEMS resonators are excited at frequencies corresponding to the induction of acoustic wave propagation, they are subjected to the deformation in different ways such as bending, twisting, or expanding [7]. The deformation mode reveals the location of nodes and antinodes of the resonator surface. Therefore, the modes exhibit the most sensitive parts of the sensor surface, which is critical for mass sensing applications. These devices can be characterized by relatively uniform mass sensitive large surface area that is vital for the longevity and sensitivity of an airborne particles micro sensor, without compromising on the device performance. For example, the resonant frequency of bulk mode resonators is not dependent on the thickness of the device. On the one hand, thick resonators result in increased area for electrostatic transduction that ultimately reducing the motional resistance in capacitively-transduced resonators. On the other hand, relatively large and thick resonators should potentially show more resistivity against harsh ambient conditions such as high wind speed and pressure. In capacitively-transduced MEMS resonators, reducing resonator-to-electrode gaps (i.e. air-gaps) lead to increase the capacitive electromechanical coupling. As a result, high signal to noise ratio and low equivalent motional impedance can be obtained.

Although the single-mask thick oxide mask layer technique has not received a lot of attention yet, it reduces the fabrication cost, complexity, and eliminates the need of removing sacrificial layer, whose thickness usually defines the size of the gaps [8] [9]. The thick oxide mask layer technique requires a selective deep-reactive ion etching (DRIE) in order to achieve high aspect ratio devices. Therefore, this method requires a thick oxide layer to sustain durable DRIE processes. At the same time, a thick oxide layer determines the final gap size by the openings of oxidized features. It has been shown that the gap aspect ratio has been achieved as high as 60:1 with this proposed technique [3]. Nevertheless, 18 µm thick SCS bulk mode MEMS resonators with a gap aspect-ratio>130 has also been achieved by using high aspect-ratio combined poly and single-crystal silicon (HARPSS) technique [6]. In this method, sacrificial oxide layer and poly silicon determines the gap size and the electrodes, respectively [10]. However, relatively simple, single-mask, and low-cost thick oxide mask layer

technique should be developed to obtain high aspect-ratio resonators. This study aims to reduce the air-gaps down to sub-µm with thick oxide mask layer technique as a conventional optical lithography method for the fabrication of bulk mode square-shaped MEMS mass sensors. In this paper, we firstly present the fabrication and optimization of high aspect ratio test structures in order to emphasize the encountered issues in this fabrication method. The latter, design, fabrication and electrical characterization of the resonators are presented.

II. HIGH-ASPECT RATIO TEST STRUCTURES OPTIMIZATION

We used test structures to optimize the relevant parameters of small gap fabrication. Firstly, a thin silicon nitride layer (~100 nm) was deposited on a silicon wafer, which was followed by a polysilicon layer deposition (~1 µm thick) (fig. 1a - I). Subsequently the designed test structures, whose feature sizes (distance between each pattern) vary from 1 µm to 25 µm, were defined by optical lithography. Then, the polysilicon layer was etched by reactive ion etching (RIE) in order to reveal the patterns (fig. 1a - II). The etched polysilicon features were thermally oxidized in an oxidation furnace at 1100°C for 3h to obtain a ~1.2 µm thick oxide layer (fig. 1a - III). Due to the silicon nitride layer, only the sidewalls and top of the polysilicon patterns were oxidized, and therefore the gap between two subsequent features was reduced to sub-µm. Finally, we used a high-aspect ratio DRIE recipe (see Table 1.) and performed the etching all the way down in the silicon wafer (fig. 1a - IV).

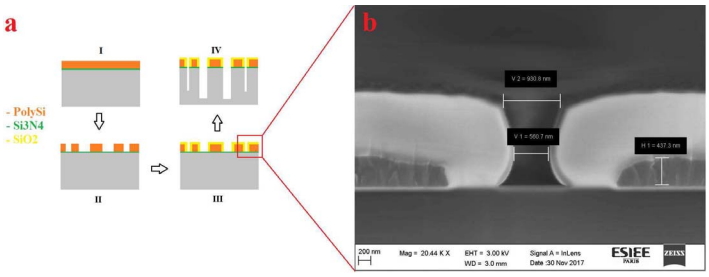

Fig. 1. Schematic of the process flow (a) and SEM image showing after ~1.2 µm oxidation of an initially ~1.7 µm spaced (after RIE etching) features (b).

TABLE I. DRIE SILICON ETCHING PARAMETERS

High-aspect ratio DRIE recipe		
Parameter	***Unit***	***Value***
Etching/Passivation	second	5/2
Flow rate : SF_6/O_2	sccm	300/150
Pressure	Pa	4
Source Power	watt	1800
LF Platen Power	watt	90
Temperature	°C	20

Following the RIE process, we measured the initial opening size in the polysilicon layer in order to determine the required thickness of the grown oxide. Several openings from ~450 nm to ~750 nm have been obtained by growing 1.2 µm oxide on different polysilicon patterns whose width vary from 1 µm to 25 µm. The initial opening was measured as ~ 1.7 µm from one of the 1 µm gap consecutive features. The non-uniform openings across the wafer are due to the resolution limit of photolithography that leads to the variations in the oxidized gaps. As the DRIE rate depends on the opening size, the depths vary from one to another consecutive feature as shown in fig. 3b. Therefore, the aspect ratio for the same openings is slightly different. For the sake of simplicity, ~70:1 gap aspect ratio was determined by taking the smallest trench width (~450 nm) and the deepest trench (~32 µm). When a high aspect ratio and vertical sidewall etching of DRIE recipe is well characterized, the aspect ratio is limited by the thickness of the oxide layer that serves as a mask layer for the selective DRIE process. In order to obtain uniform structures across the wafer, it is crucial to take the limitations of optical lithography into the account. Therefore, we designed the air-gaps as 2 µm and 1.8 µm which can be uniformly patterned across the wafer. Although the large feature size results uniform patterning, it requires a longer oxidation process for the gap reduction. However, thick oxide layer can sustain longer to DRIE process, and high-aspect ratio can therefore be obtained. As a result, this method enables high-yield fabrication of the designed sub-µm air-gap resonators.

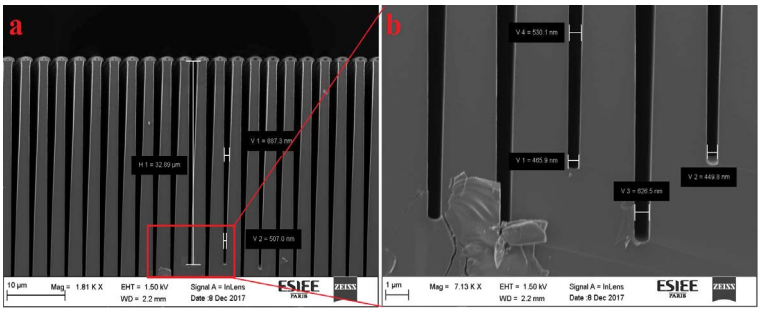

Fig. 2. SEM pictures of as small as ~465 nm wide trench with aspect ratio ~70:1. Image b represents the higher maginifation of the inset in image a.

DESIGN AND FABRICATION OF RESONANT MEMS

As demonstrated in the previous work [11], high mass sensitivity with good uniformity can be expected on square resonators operating in Lamé mode. The resonators (see table 2 and fig. 4) were designed to detect micron size particles and to resist airflow during sampling (see table 2 and fig. 4). The deformation mode was simulated in COMSOL. The t-shaped anchors (which consist of tethers and anchor beams) were optimized and placed at the edge of the resonator in order to minimize the energy loss, thereby attaining a high quality factor. It is known that the anchors can be the dominant loss mechanism by elastic wave propagation from the resonator through the anchors [12]. In this work, dimensions of the tethers and width of the anchor beams were kept constant, but the length of the anchor beams varied. In Lamé mode, shear

waves are predominate over longitudinal waves and direction of motion as expansion and contraction is equal in one axis and the orthogonal axis; thereby the volume of the structure is preserved. Typical resonance frequency of a Lamé mode resonator can be estimated as follows [12]:

$$f = \frac{1}{\sqrt{2}L}\sqrt{\frac{G}{\rho}} \quad (1)$$

Where f is the resonance frequency, L is length of the resonator, G is the shear modulus and d is the density. On the other hand, motional resistance can be defined as follows [6]:

$$R_m = \frac{d^4\sqrt{K_{eff}M_{eff}}}{Q\varepsilon^2 V_p^2 A_e^2} \quad (2)$$

Where R_m is the motional resistance, ρ is the air-gap, K_{eff} is the effective spring constant, M_{eff} is the effective mass, Q is the quality factor, Ɛ is the permittivity, V_p is the polarization DC voltage, and A_e is the effective area of the electrode. As it can be seen from the eq. 1 and 2, the resonance frequency is thickness independent in such bulk-mode resonators, and motional resistance is inversely proportional to the effective area of the resonator. Thereby, thick and small air-gap resonators lead to obtain low motional resistance (Fig. 3).

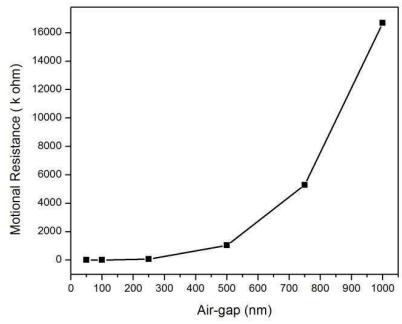

Fig. 3. Estimated motional resistance as a function of air-gap. Vdc=10V, Q =10000, $L_{electrode}$ =760 µm, $t_{electrode}$ =40 µm

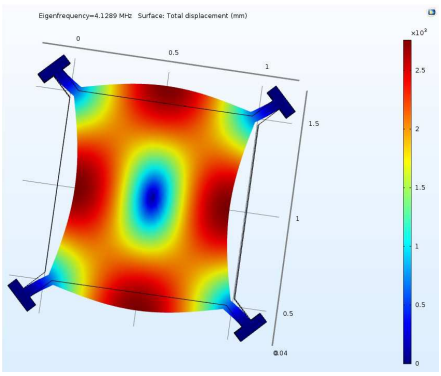

Fig. 4. COMSOL simulation results of designed Lamé mode 1mm^2 square resonator with 4.128 MHz resonance frequency.

TABLE II. DESIGNED PARAMETERS

Lamé mode square resonator		
Parameter	***Unit***	***Value***
Resonator length	µm	1000
Thickness of resonator	µm	40
Resonant frequency (1st mode)	MHz	4.1316
Effective mass	µg	46.6
Mean air-gap	nm	868
Motional resistance	k ohm	428
Length of electrodes	µm	760
Thickness of electrodes	µm	40

Since the air-gap reduction method parameters such as the smallest achievable and uniform patterning, required oxide thickness, and the DRIE recipe are well characterized, the smallest patterns were determined as 2 µm and 1.8 µm and ~1.6 µm thick oxide was grown (see fig. 5). As a result, we obtained 300 nm to 500 nm air-gaps from the 1.8 µm patterns, and 600 nm to 700 nm air-gaps from the 2 µm patterns. The latter, high-aspect ratio DRIE recipe was applied and SOI-based SCS resonators were fabricated (see fig.6-7).

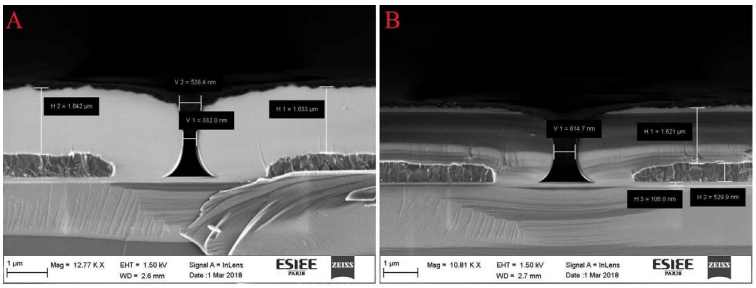

Fig. 5. SEM images shows reduced air-gaps after the oxidation of 1.8 µm patterning to 332 nm (A) and 2 µm patterning to 614 nm (B).

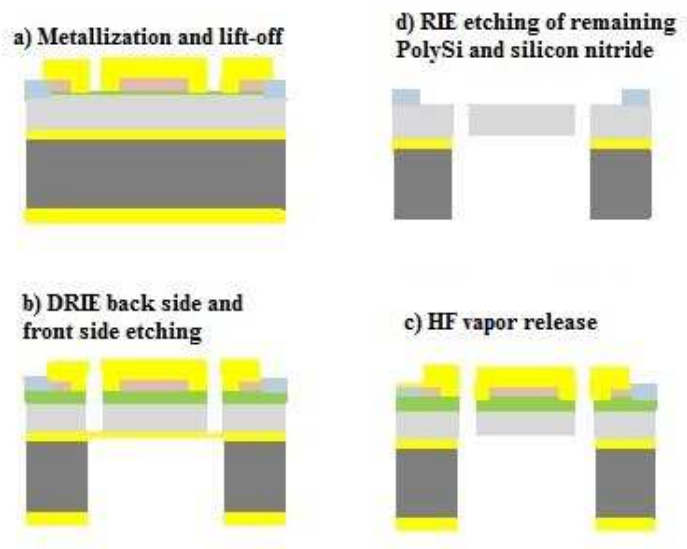

Fig. 6. Schematic of the fabrication flow shows realization of the resonator.

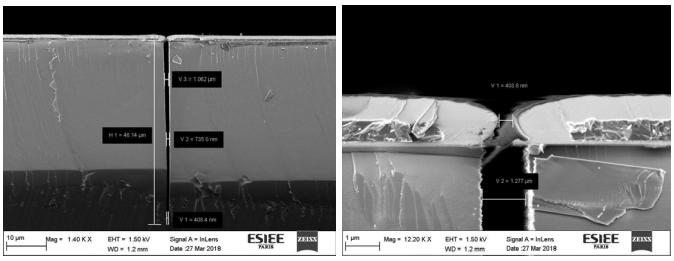

Fig.7. SEM of the high-aspect ratio sub-µm openings. The left image shows the smallest trench width as 408 nm and 46 µm depth (~115:1). The right image magnifies the opening (403 nm) of the trench.

Although the trench width reduced down to 408 nm at the bottom which is coherent with the opening after the oxidation, it is difficult to assess the aspect ratio due to non-uniform trench width along the trench depth. As it can be seen from figure 7, the trench width as large as ~ 1.3 µm begins at the top and it gets narrower by the bottom of the trench. Mean gaps as narrow as 868 nm can be obtained and the aspect ratio higher than 53:1 is achieved. In fig. 8, the top-view image of the air-gap reveals a tapered shaped-gap that hinders the feasibility of this method. The variation of the width at the top and the bottom is demanding an improved DRIE recipe in order to form relatively more vertical trenches.

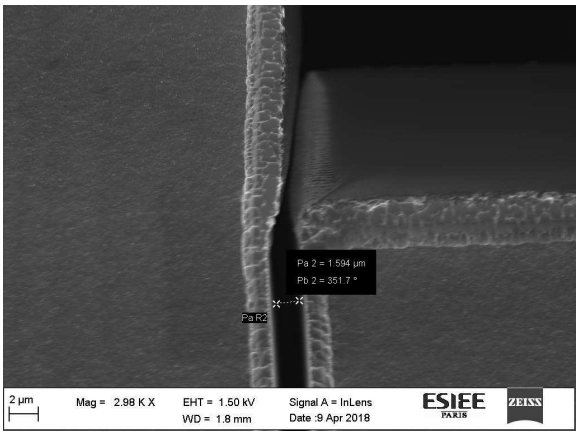

Fig.8. SEM image shows top view of the air-gap of the MEMS device. The left side of the air-gap is the resonator and the right side is the electrode.

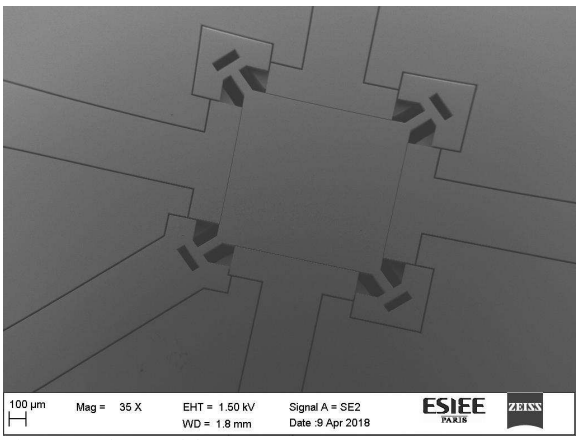

Fig.9. SEM image of the resonator.

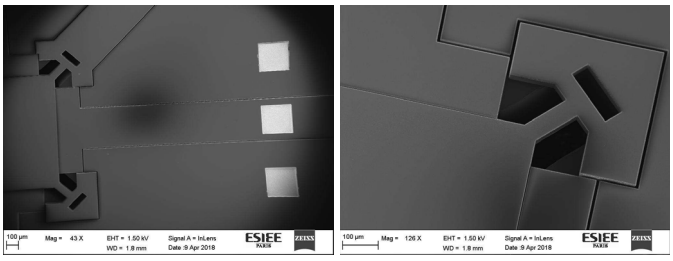

Fig.10. SEM images show the electrode and contacts (left) and the optimized T-shaped anchor of the device (right).

III. ELECTERICAL CHARACTERIZATION

The fabricated resonators were characterized by HP4194A impedanc /gain-phase analyser in air. The AC (1V) and polarization DC voltage (40V) applied to one of the electrodes, which causes periodic electrostatic force that oscilates the resonator. When the resonator vibrates at its resonance frequency where the vibration amplitude reaches its maximum, the motional AC current with the same resonance frequency can be obtained from either one of the counter electrodes or the anchors due to capacitance changes in the air-gap between the counter electrode and the resonator. In this work, preliminary electrical characterization results were obtained by using Z-probes (Signal-Ground). One of the electrodes used to excite and polarized the resonator and the motional current sensed from one of the anchors (fig. 11).

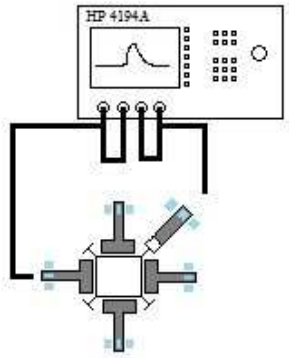

Fig.11. One-port drive and sense configuration measurement set up.

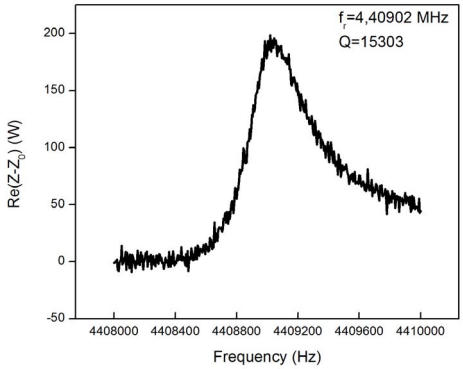

Fig.12. Mathematically compensated and measured resonance frequency response as 4.409 MHz and quality factor is estimated as 15303 at 40 V_p.

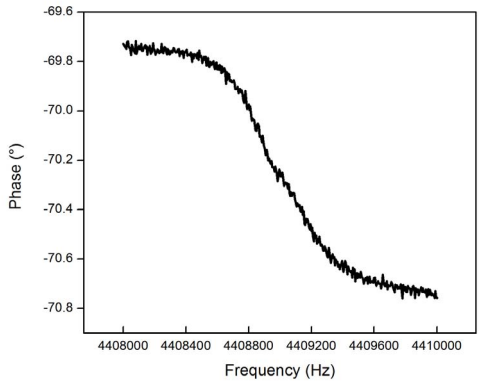

Fig.13. Mathematically compensated resonant signal, phase response at 40 V_p.

IV. CONCLUSION

High-aspect ratio bulk-mode MEMS resonators were successfully fabricated and preliminary electrical measurements were carried out. In an effort to the reduce the air-gaps to sub-µm in capacitively transduced MEMS resonators, thick oxide as a mask layer for high-aspect ratio DRIE etching method was used. The mean air-gap was reduced to ~ 868 nm while the thickness of the resonator is 40 µm. The resonance frequency of the device shown here was found to be 4.409 MHz, which is not far to the simulated Lamé mode resonance frequency (4.128 MHz). However, other devices with different anchor lengths demonstrated a resonance frequency (4.117 MHz) that closes to the fundamental Lamé mode resonance frequency. Thus, more experiments are needed to confirm this corollary. In the future work, the verticality of the trenches will be improved and the air-gap will be further reduced. The latter, mass measurements will be carried out and the mass sensors will be calibrated.

ACKNOWLEDGMENT

This work was supported by the institute Carnot – CSTB, the SATT, idf INNOV, and the DIM Analytics.

REFERENCES

[1] U. Soysal, E. Géhin, E. Algré, B. Berthelot, G. Da, and E. Robine, "Aerosol mass concentration measurements: Recent advancements of real-time nano/micro systems," J. Aerosol Sci., vol. 114, no. Supplement C, pp. 42–54, Dec. 2017.

[2] A. Cagliani and Z. J. Davis, "Ultrasensitive bulk disk microresonator-based sensor for distributed mass sensing," J. Micromechanics Microengineering, vol. 21, no. 4, p. 045016, 2011.

[3] R. Abdolvand and F. Ayazi, "A Gap Reduction and Manufacturing Technique for Thick Oxide Mask Layers With Multiple-Size Sub-mum Openings," J. Microelectromechanical Syst., vol. 15, no. 5, 1139–1144, Oct. 2006.

[4] Z. Hao, R. Abdolvand, and F. Ayazi, "A High-Q Length-Extensional Bulk-Modemass Sensor with Annexed Sensing Platforms," in 19th IEEE International Conference on Micro Electro Mechanical Systems, 2006, pp. 598–601.

[5] J. E.-Y. Lee, Y. Zhu, and A. A. Seshia, "A bulk acoustic mode single-crystal silicon microresonator with a high-quality factor," J. Micromechanics Microengineering, vol. 18, no. 6, p. 064001, 2008.

[6] S. Pourkamali and F. Ayazi, "High frequency capacitive micromechanical resonators with reduced motional resistance using the HARPSS technology," in Digest of Papers. 2004 Topical Meeting onSilicon Monolithic Integrated Circuits in RF Systems, 2004., 2004, pp. 147–150.

[7] H. Campanella, Acoustic Wave and Electromechanical Resonators: Concept to Key Applications. Artech House, 2010.

[8] N. D. B. Ciressan, C. Hibert, M. Mazza, and A. M. Ionescu, "Fabrication of silicon-on-insulator MEM resonators with deep sub-micron transduction gaps," Microsyst. Technol., vol. 13, no. 11–12, 1489–1493, Jul. 2007.

[9] S. Pourkamali and F. Ayazi, "SOI-based HF and VHF single-crystal silicon resonators with SUB-100 nanometer vertical capacitive gaps," in TRANSDUCERS, Solid-State Sensors, Actuators and Microsystems, 12th International Conference on, 2003, 2003, vol. 1, pp. 837–840 vol.1.

[10] F. Ayazi and K. Najafi, "High aspect-ratio combined poly and single-crystal silicon (HARPSS) MEMS technology," J. Microelectromechanical Syst., vol. 9, no. 3, pp. 288–294, Sep. 2000.

[11] B. Berthelot, E. Algré, S. Moularat, E. Robine, and E. Gehin, "Design optimisation of silicon-based MEMS sensors dedicated to bioaerosols monitoring," in *2015 Symposium on Design, Test, Integration and Packaging of MEMS/MOEMS (DTIP)*, 2015, pp. 1–5.

[12] L. Khine, M. Palaniapan, and W. K. Wong, "12.9MHz Lame-Mode Differential SOI Bulk Resonators," in *TRANSDUCERS 2007 - 2007 International Solid-State Sensors, Actuators and Microsystems Conference*, 2007, pp. 1753–1756.